JOURNAL OF MATERIALS SCIENCE 25 (1990) 1664–1674

The flexural strength and microhardness of $YBa_2Cu_3O_{6+\delta}$

MARK K. IHM
Materials Testing Laboratory, Chevrolet–Pontiac–General Motors of Canada, Warren, Michigan 48090, USA

BOB R. POWELL*, RAYMOND L. BLOINK
Metallurgy Department, General Motors Research Laboratories, Warren, Michigan 48090–9055, USA

The flexural strengths of rectangular $YBa_2Cu_3O_{6+\delta}$ bars, prepared from mixed oxides and carbonates or spray-dried precursors, have been measured at room temperature and at 77 K. Strengths ranged from 17.8 to 57.6 MPa at room temperature, depending on processing history, and were 20% greater when measured at 77 K. Corrosion of $YBa_2Cu_3O_{6+\delta}$ in humid air at 38° C created two layers of corrosion products, but did not weaken the uncorroded core when failure loads were corrected for the decreased sample dimensions. The Knoop hardness of polycrystalline $YBa_2Cu_3O_{6+\delta}$ ranged from 436 to 447 KHN while the hardness of individual grains of $YBa_2Cu_3O_{6+\delta}$ was 498 KHN. Variations in flexural strength with microstructure were observed and are discussed.

1. Introduction

The discovery of ceramic materials that superconduct at temperatures above 77 K, the boiling point of liquid nitrogen, has prompted considerable interest in superconducting devices such as motors and generators [1]. One issue that will influence the successful application of ceramic superconductors in such devices is their mechanical reliability under the necessary operating conditions. For example, some design concepts for superconducting motors expose the ceramic to high tensile stresses during motor start-up and during high-speed rotation. The ceramic could also be exposed to frictional wear and corrosion at the electrical contacts. Unfortunately, little is known about the mechanical properties of $YBa_2Cu_3O_{6+\delta}$. Results to date [2] indicate that $YBa_2Cu_3O_{6+\delta}$ is very brittle with reported fracture toughnesses of 1.3 MPa $m^{1/2}$ for polycrystalline $YBa_2Cu_3O_{6+\delta}$ and 1.1 MPa $m^{1/2}$ for single crystals. This value is similar to that of fibreglass. $YBa_2Cu_3O_{6+\delta}$ has also been reported to be susceptible to slow crack growth [2].

The object of this study was to measure the flexural strength and microhardness of $YBa_2Cu_3O_{6+\delta}$ prepared by a variety of procedures and to relate these properties to sample microstructure.

2. Experimental procedure

2.1. Sample preparation

$YBa_2Cu_3O_{6+\delta}$ powders were prepared from spray-dried solutions of yttrium, barium and copper salts or from mixtures of the metal oxides and carbonates. A summary of the powder preparation conditions and subsequent processing conditions is shown in Table I.

The first set of bars, identified as 35A, was prepared from a spray-dried aqueous solution of yttrium acetate, barium acetate and copper nitrate. This solution was prepared by dissolving yttrium acetate in distilled water by adding concentrated nitric acid and then by adding appropriate amounts of barium acetate and copper nitrate stock solutions to yield a Y : Ba : Cu atom ratio of 1 : 2 : 3. Spray-drying consisted of atomizing the solution in a chamber of hot, swirling air. The dried and partially decomposed salts were carried in the air stream through the outlet of the chamber and collected in a cyclone filter. The inlet and outlet temperatures during spray-drying were 180 and 90° C, respectively. Spray-drying yielded a solid product that was then calcined at 850° C for 12 h in flowing, hydrocarbon-free air. Chemical analysis of the calcined powder showed that the Y : Ba : Cu atom ratio was still 1.0 : 2.0 : 3.0. This powder was uniaxially pressed at 41 MPa into test bars and sintered in flowing, hydrocarbon-free air at 950° C for 6 h. A total of 36 bars were made.

Of these bars, two sets of twelve were set aside for flexural strength testing at room temperature and 77 K, respectively. The remaining twelve bars were put into a humidity chamber for 100 h. In the chamber the bars were exposed to an atmosphere of air at 38° C and a relative humidity of 100%.

The second set of bars, 53A, was prepared by calcining a mixture of barium carbonate, yttrium oxide and copper oxide. As before, the reagents were combined to give a Y : Ba : Cu atom ratio of 1 : 2 : 3. This mixture was calcined at 950° C for 39 h, ground with a mortar and pestle, and calcined an additional 39 h. After

*To whom all correspondence should be addressed.

0022–2461/90 $03.00 + .12

cooling, the powder was ball-milled for 15 h using zirconia balls and toluene. Since the resulting powder was still coarse, the powder was dry-milled for an additional 48 h. Chemical analysis of the powder indicated an atom ratio of 1.0 : 1.9 : 3.1. Test bars were uniaxially pressed from the powder after addition of ~ 1 wt % polyvinyl alcohol to aid in compaction. The bars were then sintered at 950° C for 6 h in a muffle furnace.

The third set of samples was prepared by spray-drying a solution containing nitrate salts of yttrium, barium and copper. The solution was spray-dried using an inlet temperature of 350° C and an outlet temperature of 140° C. The resulting powder was calcined at 850° C for 6 h in flowing, hydrocarbon-free air. Analysis of the calcined powder revealed a Y : Ba : Cu atom ratio of 1.0 : 2.0 : 3.0. The powder was then pressed into two sets of 12 bars. The first set, 53B, was uniaxially pressed and subsequently sintered at 950° C for 6 h in a muffle furnace. The second set, 54C, was uniaxially pressed at 41 MPa, cold-isostatically pressed at 310 MPa, and sintered at 950° C for 6 h in a muffle furnace.

Superconductivity was verified by placing some of the bars from each set in liquid nitrogen and observing the Meissner effect, i.e. the expulsion of a magnetic field by the $YBa_2Cu_3O_{6+\delta}$ [3]. All of the bars tested, including the bars removed from the humidity chamber, exhibited superconductivity in this manner.

2.2. Mechanical testing

Samples for flexural strength testing were prepared in the form of sintered bars having nominal dimensions of 2 mm by 3 mm by 40 mm. The broken pieces of the bars were used for microhardness testing and material characterization. The sintered bars were prepared for flexural strength tests by hand-finishing in the direction of the long axis with 400 grit paper followed by 600 grit paper. Several of the bars from sets 35A, 53A and 53B broke during the finishing. It was decided to prepare these sets with a very light 400 grit sanding only. The bars that had been exposed to the humidity chamber received no surface preparation other than the removal of two layers of corrosion products which were loosely attached to the bars.

Flexural strength tests were performed using a four-point loading method according to Military Standard 1942A [4]. A silicon carbide, four-point fixture with an upper span of 10 mm and a lower span of 20 mm was used. Testing was performed on a Satec universal testing machine, and a crosshead speed of 0.2 mm min^{-1} was employed. The strength of a beam in four-point flexure was calculated using the fomula

$$S = \frac{3PL}{4bd^2}$$

where P is the failure load, L the outer support span of the testing fixture, b the specimen width and d the specimen thickness. Both b and d were measured at the point of fracture. Ten bars were tested from each set of samples.

Samples were prepared for microhardness measurements by mounting and polishing transverse sections from test bars. Polishing consisted of 320, 600 and 1200 grit finishing with dry sandpaper followed by 6 μm and 1 μm diamond polishing steps. In between the diamond polishes, a quick soap and cold water rinse was performed. Hardness was measured using a Tukon microhardness tester with Knoop indenter. A Knoop indenter was chosen over a Vickers' diamond pyramid indenter because the Knoop indenter does not penetrate as deeply into the surface as the Vickers' indenter, thereby causing less cracking around the indentations. A load of 200 g was chosen to minimize the cracking associated with hardness indentations while maintaining a small effect of elastic recovery in the material [5]. Hardness measurements of single grains were made on a sample from set 35A, identified as 35A(HT), which had been heat-treated in air at 975° C for 100 h to obtain very large grains.

2.3. Material characterization

Material characterization included X-ray diffraction analysis, density determination, microprobe analysis

TABLE I Preparation methods of $YBa_2Cu_3O_{6+\delta}$ sample sets

Sample set	No. of bars	Powder preparation	Calcining		Powder compaction	Sintering	
			Temp. (° C)	Time (h)		Temp. (° C)	Time (h)
35A	36	Spray-dried from an aqueous solution of yttrium acetate, barium acetate and copper nitrate	850	12	Pressed into bars	950	6
53A	12	Calcined and milled mixture of yttrium oxide, copper oxide and barium carbonate	950	78	Pressed into bars with polyvinyl alcohol added	950	6
53B	12	Spray-dried from an aqueous solution of yttrium nitrate, barium nitrate and copper nitrate	850	6	Pressed into bars	950	6
54C	12	Spray-dried from an aqueous solution of yttrium nitrate, barium nitrate and copper nitrate	850	6	Pressed into bars and isostatically pressed at 310 MPa	950	6

and fracture analysis. Several pieces from each set of bars and pieces of the corrosion products from the humidity test were ground and characterized by X-ray diffraction using a Siemens D500 X-ray diffractometer. Other pieces of the bars were used for density measurements. The densities of these pieces were determined by the Archimedes method.

Fracture surfaces from each set of bars were examined using an Amray 1000B scanning electron microscope equipped with a Tracor Northern wavelength-dispersive spectrometer. Several pieces of the bars from all the sets were mounted and polished for microstructural analysis. The polishing procedure was the same as that used to prepare samples for microhardness measurements. The microstructure of these samples was observed using double-polarized light on a Reichert–Jung metallograph.

Polished samples from set 54C were analysed using a Cameca MBX electron microprobe to determine the extent to which other phases were present in the microstructure. A polished cross-section of a humidity-exposed sample was analysed to determine the phases present at the corrosion interface.

3. Results and discussion

An attempt has been made to obtain a broad view of the mechanical properties of $YBa_2Cu_3O_{6+\delta}$ and the variability of those properties. Flexural strength and microhardness measurements were made at room temperature for $YBa_2Cu_3O_{6+\delta}$ samples prepared by a variety of methods. Flexural strength measurements were also made in liquid nitrogen since this is the thermal environment under which the superconductor will operate. Finally, the corrosion behaviour and its effect on the flexural strength of $YBa_2Cu_3O_{6+\delta}$ were determined to assess the need for controlling the operating environment of the superconductor. In this section each of these experimental results is presented and discussed.

3.1. Flexural strength

The average flexural strengths for the sample sets are presented in Table II. The average room-temperature strengths for the sample sets tested in this study ranged from 17.8 ± 2.8 to 57.6 ± 3.2 MPa. The differences in strength among the sample sets and the possible influences of phase purity, density and grain size will be discussed later. The observed strengths for $YBa_2Cu_3O_{6+\delta}$ are in the low range for typical ceramic materials. Pyrex and fused silica have strengths of 70 MPa, hot-pressed boron nitrate fractures at between 50 and 100 MPa, and sintered alumina has reported strengths greater than 350 MPa [6].

Flexural strengths of 216 and 115 MPa have been reported for $YBa_2Cu_3O_{6+\delta}$ by Alford *et al.* [7] and Blendell *et al.* [8], respectively. These values are not directly comparable to the results reported in our study for several reasons. First, the reported test samples were either cylinders [7] or rectangular bars with rounded edges [8], whereas our samples were rectangular with sharp edges. Cylinders and bars with rounded edges have smaller stressed volumes during testing than do the rectangular bars, which effects a greater apparent strength in the cylindrical or rounded test bars. Both sets of samples had smaller overall dimensions than the rectangular bars tested in this study. The differences in the stressed volumes between the two sample geometries, and the fact that the cylinders and rounded bars were tested in three-point fixtures instead of a four-point fixture, would tend to overestimate the strength of the cylinders by about 60% [9]. Furthermore, the loading rate for testing of both literature samples was 5 mm min^{-1}, 25 times greater than the loading rate used in this study. The higher loading rate would increase the apparent strength of the samples by about 20% [9] although the increase may even be greater since $YBa_2Cu_3O_{6+\delta}$ is susceptible to slow crack growth. These factors suggest that corrected flexural strengths of less than 110 MPa for the Alford *et al.* samples and 60 MPa for the Blendell *et al.* samples would be more properly compared with our test results.

Patel *et al.* [10] have measured the compressive strength of $YBa_2Cu_3O_{6+\delta}$ at 80 and 93% of theoretical density. As expected it is much larger than the flexural strengths observed in this study. The 80% dense

TABLE II Mechanical properties of $YBa_2Cu_3O_{6+\delta}$ sample sets

Sample set	Flexural strength tests			Microhardness tests	
	Testing conditions	Average flexural strength (MPa)	Standard deviation (%)	Average hardness (KHN)	Standard deviation (%)
35A	Tested at room temperature in air	33.8	5.3	437	3.5
	Tested at 77 K in liquid nitrogen	40.1	7.4		
	Tested at room temperature in air after a soak of 100 h in humid air at 38° C	33.6	6.6		
35A(HT)*				498	7.7
53A	Tested at room temperature in air	23.7	4.2		
53B	Tested at room temperature in air	17.8	15.8		
54C	Tested at room temperature in air	57.6	5.5	447	4.3

*Sample from set 35A which was heat-treated to obtain very large grains for hardness measurements of individual grains.

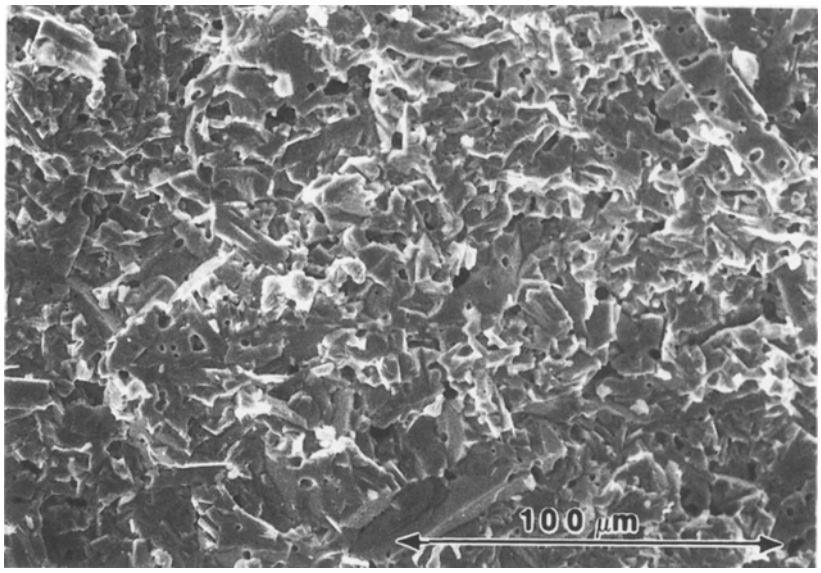

Figure 1 Scanning electron micrograph showing fracture surface of bar from set 35A tested at room temperature (500×).

$YBa_2Cu_3O_{6+\delta}$ failed at 184 MPa while the 93% dense sample, which contained calcium as a sintering aid, failed at 287 MPa. Because of its relatively low strength, superconductor device designs that place $YBa_2Cu_3O_{6+\delta}$ in tension should be avoided by using $YBa_2Cu_3O_{6+\delta}$ in non-rotating parts or by compression-fitting it into stronger containers.

When the flexural strengths of test bars from sample set 35A were measured in liquid nitrogen, the strength increased by nearly 20% relative to the room-temperature strength; 40.1 ± 3.0 as against 33.8 ± 1.8 MPa. Figs 1 and 2 show that the fracture surfaces obtained from room-temperature and 77 K measurements are the same. The observed increase in the flexural strength at 77 K compares favourably with the observation of Patel *et al.* [10] that the compressive strength of $YBa_2Cu_3O_{6+\delta}$ increased from 184 to 231 MPa (approximately 25%) when tested at room temperature and 77 K, respectively.

3.2. Effect of humidity treatment on flexural strength

Another issue for the utilization of $YBa_2Cu_3O_{6+\delta}$ superconductors is their reported susceptibility to moisture [11]. Twelve bars of 35A $YBa_2Cu_3O_{6+\delta}$ material were put in a humidity chamber for 100 h to observe how $YBa_2Cu_3O_{6+\delta}$ reacts to this type of environment. After removal from the humidity chamber, the bars exhibited a white powdery layer on the surface (Fig. 3). This white layer fell off intact, revealing a black layer which also came off intact. These two layers were set aside for analysis. The flexural strength of the bars was then measured. The flexural strength results are shown in Table II.

The failure loads of the bars were lower than those of the untreated bars. However, calculating the flexural strength using the smaller cross-sectional dimensions showed that the strength of the humidity-tested bars was similar to the strength of bars that were tested at room temperature but had not been exposed to the humidity treatment (set 35A). On a Weibull plot the two sets of test results were indistinguishable. The fracture morphologies of the bars shown in Fig. 4 were similar to those tested at room temperature (Fig. 1) except at the surface, where some of the corrosion products remained. Thus the bulk, uncorroded core did not appear to have been weakened by any penetration of water into the material either along grain boundaries or through the lattice.

Fig. 5 shows the diffraction patterns for bars before

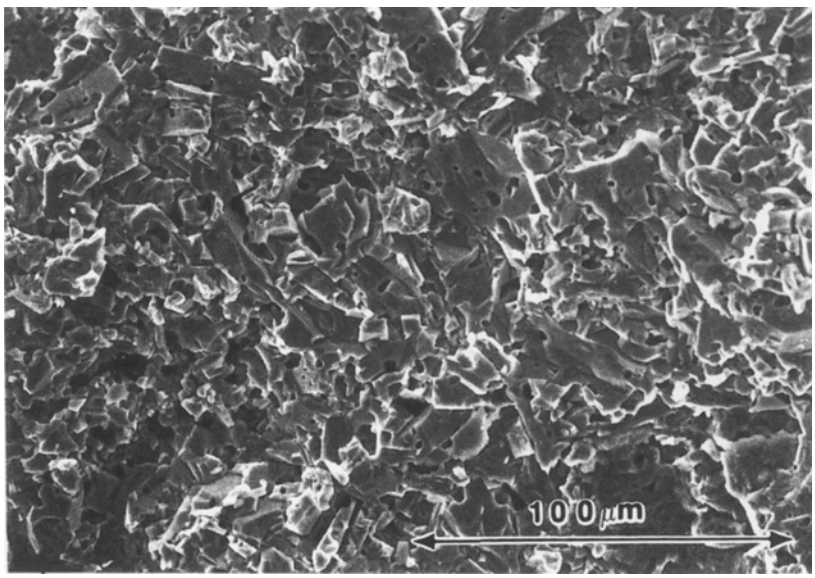

Figure 2 Scanning electron micrograph showing fracture surface of bar from set 35A tested in liquid nitrogen (77 K) (500×).

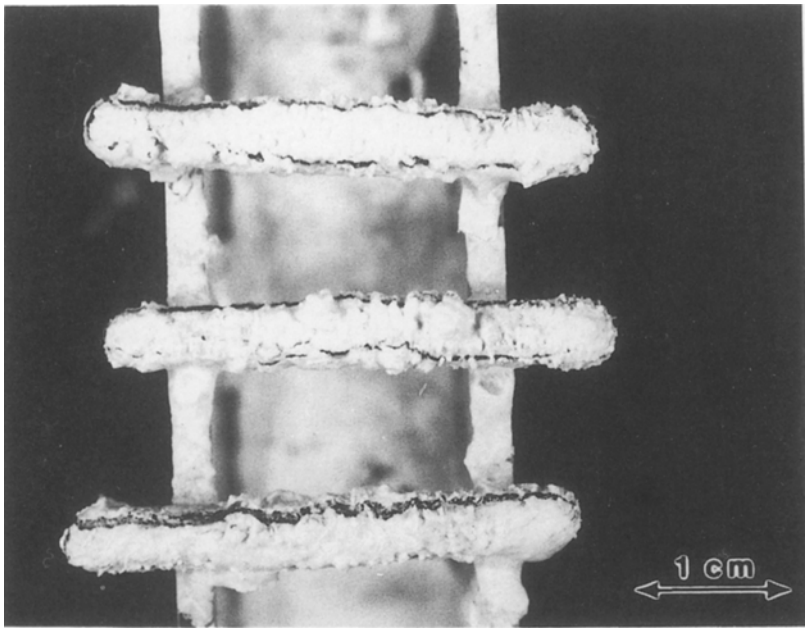

Figure 3 Optical micrograph of three test bars after removal from humidity chamber. A white $BaCO_3$ corrosion layer covers each bar (2×).

the humidity treatment and also for the white corrosion layer, the black corrosion layer, and the core of the test bars after the humidity treatment. The white layer is composed of $BaCO_3$, and the black layer is composed of $BaCO_3$, CuO and Y_2BaCuO_5. The core of the test bars after treatment in the humidity chamber shows mostly $YBa_2Cu_3O_{6+\delta}$ with some Y_2BaCuO_5 and $BaCuO_2$. Microprobe analysis of the reaction zone at the surface of the bars shows CuO, Y_2BaCuO_5 and $YBa_2Cu_3O_{6+\delta}$, (Fig. 6). This is consistent with the literature which suggests the following reactions between $YBa_2Cu_3O_{6+\delta}$ and water and carbon dioxide [11]:

$$2YBa_2Cu_3O_{6+\delta} + 3H_2O$$
$$\rightarrow Y_2BaCuO_5 + 3Ba(OH)_2 + 5CuO + 0.5O_2$$
$$Ba(OH)_2 + CO_2 \rightarrow BaCO_3 + H_2O$$

The layer of $BaCO_3$ at the surface of the test bars is probably the result of $Ba(OH)_2$ leaching to the surface and reacting with carbon dioxide.

In this study these reactions took place at 38° C. It is not known whether $YBa_2Cu_3O_{6+\delta}$ is susceptible to this type of corrosion at temperatures below its superconducting transition temperature. However, one would expect that corrosion would proceed more slowly due to the slower kinetics of ice compared with water and the lower water vapour concentration in the cold gases around the superconductor (assuming that $YBa_2Cu_3O_{6+\delta}$ is not a condensation site for ambient air).

3.3. Influence of microstructure on flexural strength

Several microstructural factors are known to influence the strength of ceramics. These include density, grain size, and phase purity, i.e. the presence of small amounts of second phases. A plot of flexural strength against density is shown in Fig. 7. While ceramics generally become stronger as density increases, that trend is not evident in the figure. However, microstructural analysis of the samples does provide some clarification of these test results.

Table III gives a summary of the materials properties of the five sets of bars. X-ray diffraction patterns for the five sample sets, presented in Figs 5 and 8,

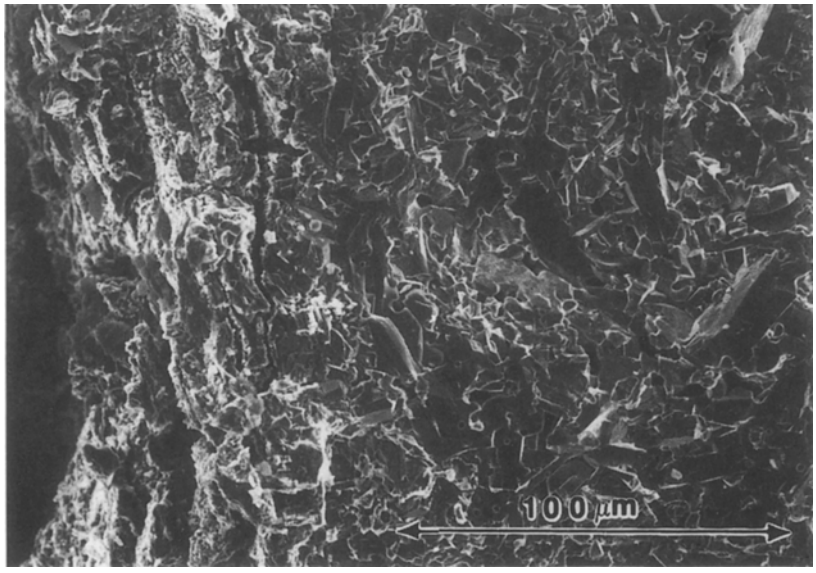

Figure 4 Fracture surface of a humidity-treated test bar from set 35A. Corroded surface is on left side of micrograph (500×).

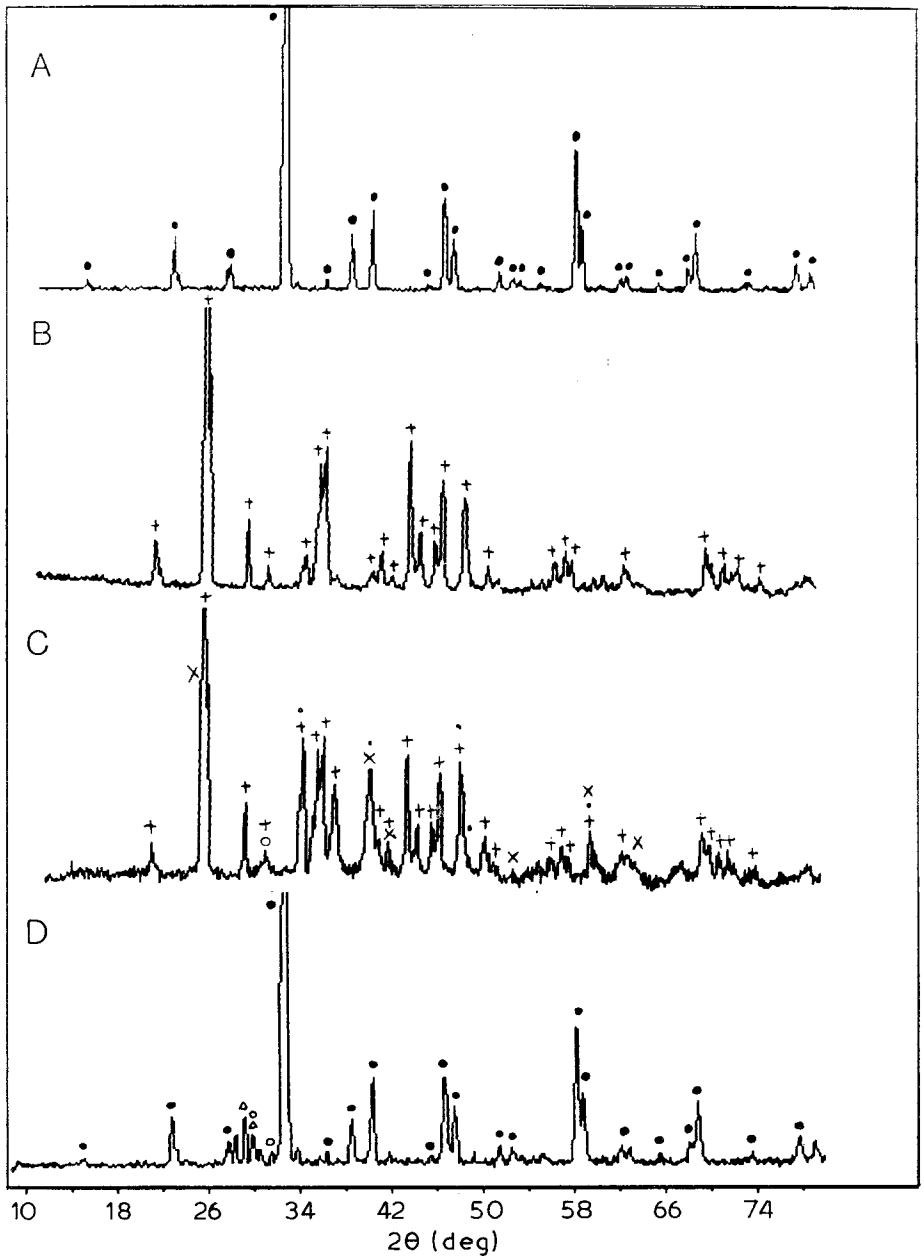

Figure 5 Effect of humidity treatment on $YBa_2Cu_3O_{6+\delta}$ from set 35A. X-ray spectra are of (A) bars prior to humidity treatment, (B) the white corrosion layer, (C) the black near-surface corrosion layer, and (D) the "uncorroded core". (●) $YBa_2Cu_3O_{6+\delta}$, (+) $BaCO_3$, (x) CuO, (○) Y_2BaCuO_5, (△) $BaCuO_2$.

show that while $YBa_2Cu_3O_{6+\delta}$ is the major phase, some of the sets had additional phases present in the material. The bars from sets 53B and 54C show small amounts of second phases such as $BaCuO_2$ and Y_2BaCuO_5. With respect to phase purity, sets 35A and 53A are the purest while sets 53B and 54C, which were prepared from the same starting material, are the poorest. Within each set, the higher-density sample set shows the greater strength. Regarding the greater strength of set 54C relative to set 53B, it is to be noted that the only difference between these samples was that the bars in set 54C were cold-isostatically pressed to 310 MPa prior to sintering. It is possible that additional phases contribute to strengthening

TABLE III Materials properties of $YBa_2Cu_3O_{6+\delta}$ sample set

Sample set	Density measurements			Fracture appearance	Phase and distribution	Grain size (μm)*
	Average bulk density ($g\,cm^{-3}$)	Average apparent density ($g\,cm^{-3}$)	Percentage bulk density (%)			
35A	5.59	6.04	88	Mostly transgranular with some intergranular features	$YBa_2Cu_3O_{6+\delta}$ throughout	16 ± 5
53A	5.26	6.43	83	Transgranular and intergranular features	$YBa_2Cu_3O_{6+\delta}$ throughout	45 ± 5
53B	3.72	6.25	58	Transgranular and intergranular features	$YBa_2Cu_3O_{6+\delta}$ with patches of Y_2BaCuO_5 and $BaCuO_2$	< 11 ± 3
54C	4.80	6.26	76	Transgranular and intergranular features	$YBa_2Cu_3O_{6+\delta}$ with $BaCuO_2$ dispersed evenly throughout	11 ± 3

*Measured by comparison with ASTM grain size charts according to ASTM E112 [12].

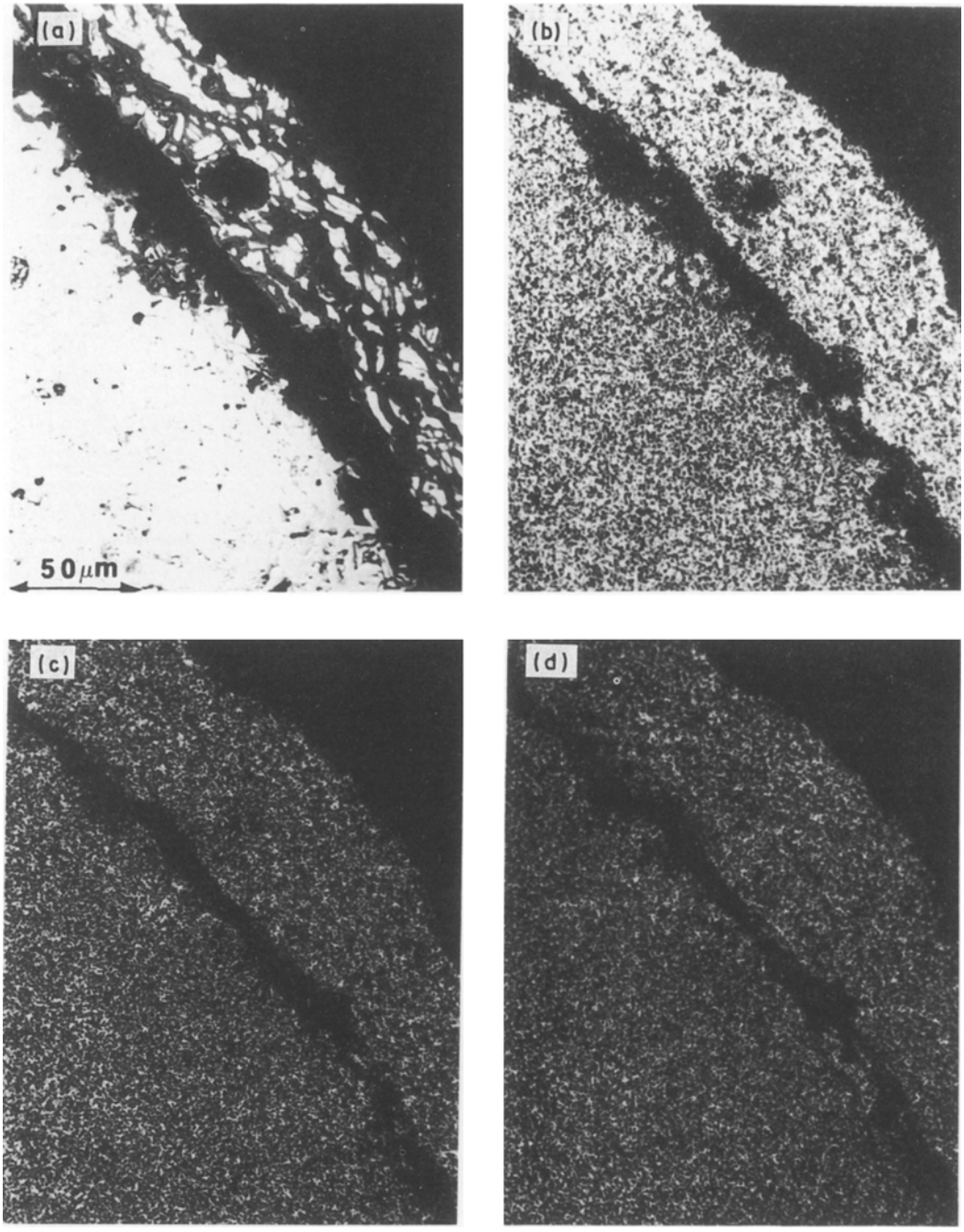

Figure 6 Electron microprobe analysis of 35A bar after humidity treatment. Micrographs are (a) the backscattered electron image and elemental maps for (b) yttrium (c), barium and (d) copper. All magnifications are 400×.

$YBa_2Cu_3O_{6+\delta}$, but this cannot be demonstrated with these data.

Grain size can also influence mechanical strength. Grain size determinations were made for each sample set by the comparison procedure in ASTM E112-85 [12]. The results are contained in Table III. A set of optical micrographs, using double-polarized light and all at the same magnification, is shown in Fig. 9. Sample sets 53B and 54C, which were prepared from the same spray-dried precursor and have approximately the same degree of phase purity, also have the same very fine grain size. A comparison of Figs 10 and 11 shows that neck growth, i.e. grain boundary formation, is more extensive in the cold-isostatically pressed samples from set 54C than in sample set 53B which was prepared without cold-isostatic pressing. This probably explains the low strength and intergranular fracture behaviour of set 53B compared to the high strength and intragranular fracture behaviour of set 54C.

The $YBa_2Cu_3O_{6+\delta}$ grains in set 53A are much coarser than the grains in the other single-phase sample set, 35A. This is understandable considering that 53A was made from calcined mixtures of oxides and carbonate while 35A was prepared from spray-dried precursor. In this comparison the finer grain size and higher density may contribute to the greater flexural strength of sample set 35A.

3.4. Microhardness

Many design concepts for superconducting motors expose the ceramic to frictional wear at electrical brush contacts. The wear behaviour at these contacts may determine the feasibility of the motor design. The

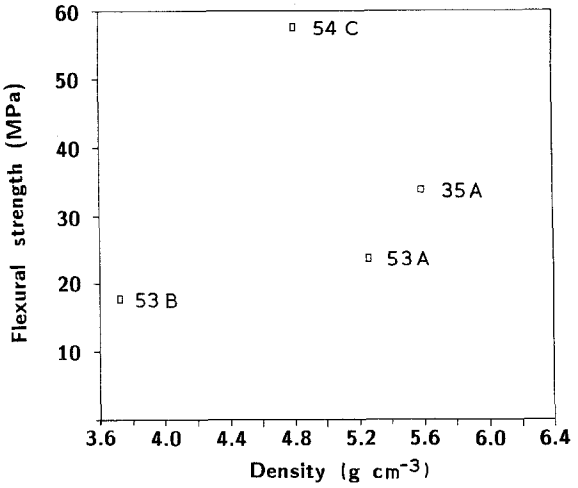

Figure 7 Plot of flexural strength of $YBa_2Cu_3O_{6+\delta}$ samples against sample density. Individual sample sets are labelled in the figure.

wear resistance of a ceramic can often be related to the material's hardness. Results reported to date show the hardness of polycrystalline $YBa_2Cu_3O_{6+\delta}$ to be about 2.0 GPa using a Vickers diamond pyramid hardness indenter [10].

The Knoop microhardness results obtained for $YBa_2Cu_3O_{6+\delta}$ in this work are shown in Table II. While Knoop hardness numbers do not convert directly to Vickers hardness numbers, 440 KHN (which is representative of the results obtained in this work) corresponds to 4.3 GPa which is somewhat higher than the Vickers hardness previously reported [10]. Hardness measurements of samples 53A and 53B were not taken due the difficulty of preparing a sufficient polish on these samples. There is no significant difference among the hardness values observed, with the exception of 35A(HT). This sample was annealed to increase the grain size in order to make measurements on single grains. In this sample, the hardness indentations on the large, single grains exhibited some cracking, but most of this cracking was contained within the grains (Fig. 12). The result was that the hardness of individual grains was 498 KHN compared with ~440 KHN for the other samples.

4. Further observations

In this study, the mechanical properties of $YBa_2Cu_3O_{6+\delta}$ have been determined for samples prepared in several different ways and general trends such as increasing strength with increasing density have been observed. The data reported herein and elsewhere should be of use when designing superconducting devices. However, the mechanical properties are likely to improve as the processing of $YBa_2Cu_3O_{6+\delta}$ becomes better understood.

Among the improvements in microstructure that should accompany evolving processing science will be higher density and finer grain size, both of which generally increase the strength of ceramic materials. However, while high density and fine grain size may be desirable from a mechanical properties point of view, these properties may not be desirable in $YBa_2Cu_3O_{6+\delta}$. Superconductivity in $YBa_2Cu_3O_{6+\delta}$ is very sensitive to

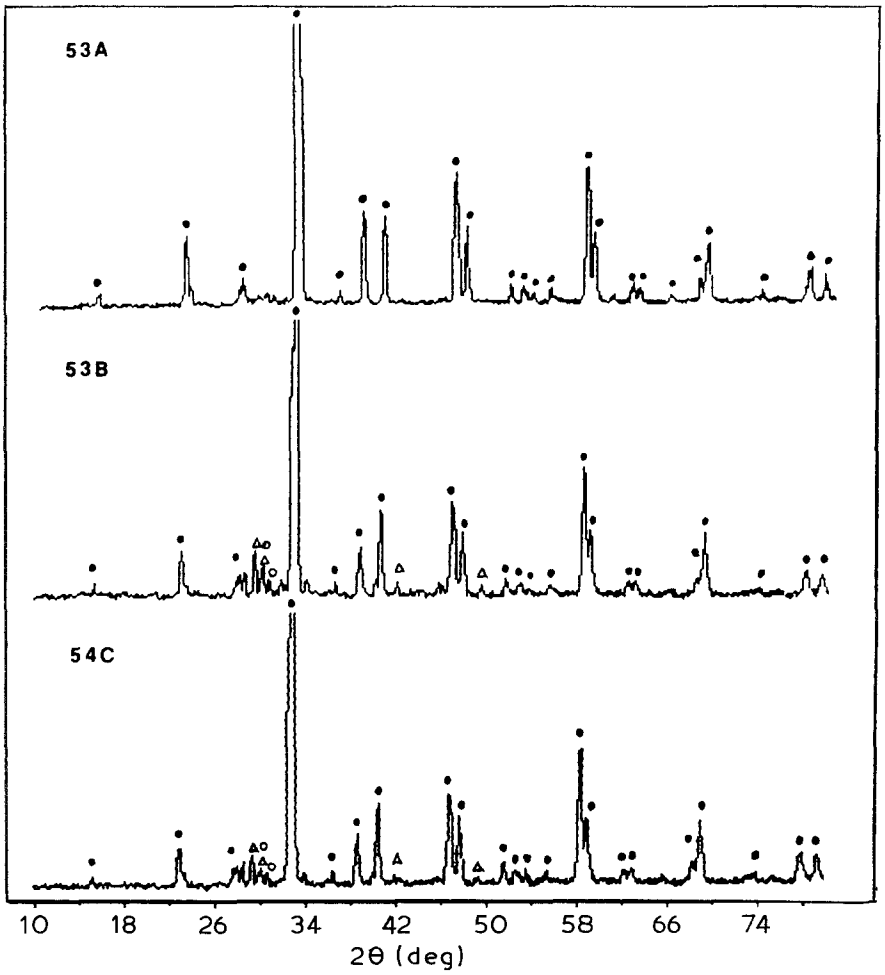

Figure 8 X-ray diffraction spectra from samples 53A, 53B and 54C. (●) $YBa_2Cu_3O_{6+\delta}$, (○) Y_2BaCuO_5, (△) $BaCuO_2$.

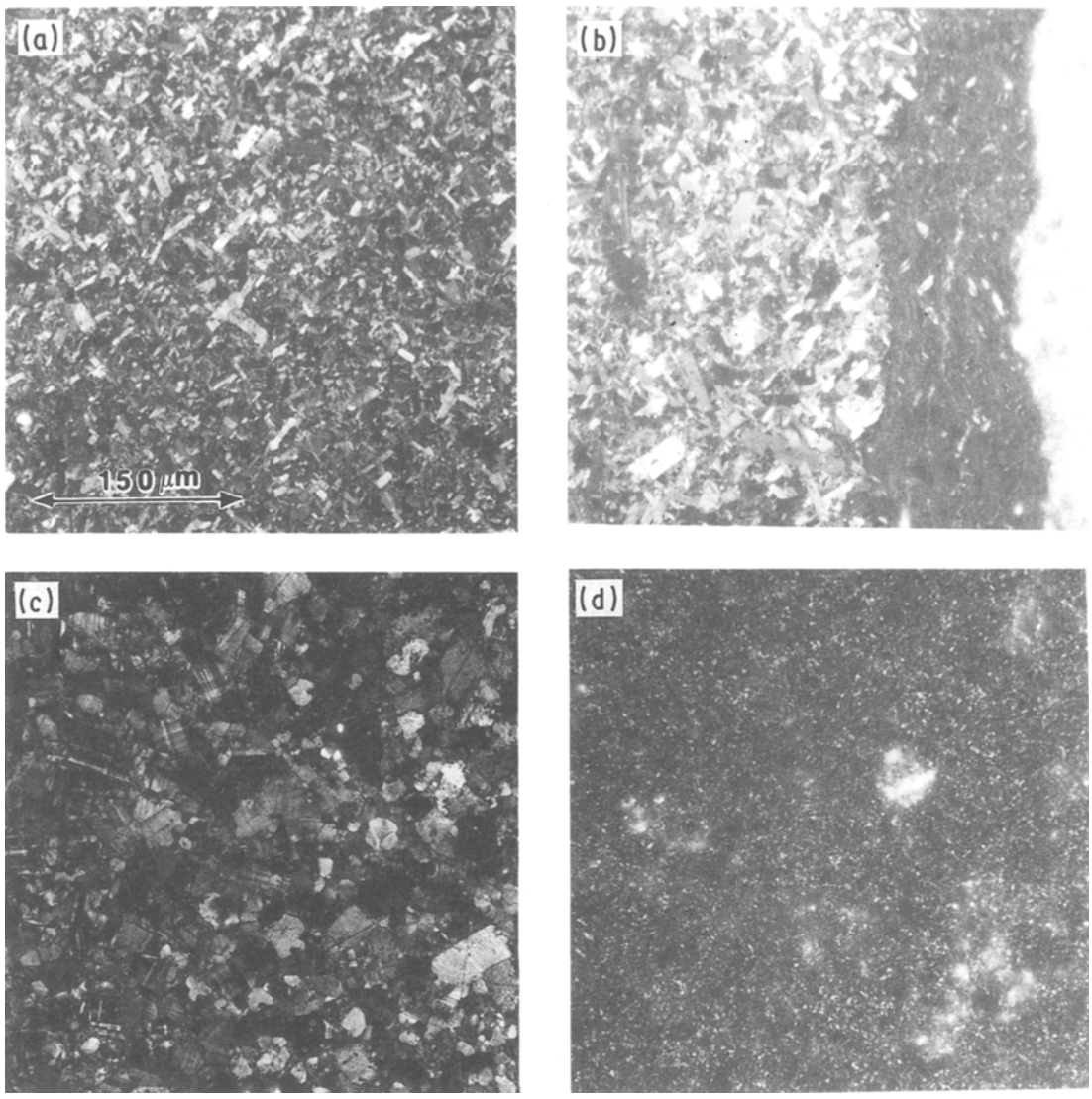

Figure 9 Optical micrographs showing grain size of (a) 35A, (b) 35A after humidity treatment, (c) 53A, (d) 53B and (e) 54C. All magnifications are × 200.

oxygen stoichiometry, a stoichiometry that is destroyed during densification at high temperatures (above 700° C). The result is that restoration of the oxygen stoichiometry in dense samples must be achieved by a low-temperature (400 to 600° C) annealing treatment. As the density of $YBa_2Cu_3O_{6+\delta}$ is increased above 90%, the open-pore network collapses into closed pores thereby requiring that oxygen diffusion into the bulk occur by lattice diffusion, a very slow process. A fine grain size may also be detrimental to superconductivity in $YBa_2Cu_3O_{6+\delta}$. Studies have shown that the critical current density in $YBa_2Cu_3O_{6+\delta}$ single crystals approaches $10^6\,A\,cm^{-2}$ [13]. The highest reported critical current density in polycrystalline $YBa_2Cu_3O_{6+\delta}$ is $7400\,A\,cm^{-2}$ [14]. This difference is generally attributed to the presence of grain boundaries [15] which become more numerous as the grain size becomes finer.

For the above reasons, it may be necessary to balance the mechanical properties of $YBa_2Cu_3O_{6+\delta}$ with the necessary superconducting properties. Methods of strengthening $YBa_2Cu_3O_{6+\delta}$ superconductors have been suggested which include the introduction of second phases such as ceramic whiskers and fibres or the fabrication of layered composites [2, 16]. In any event, tailoring of the microstructure of $YBa_2Cu_3O_{6+\delta}$ continues to be a substantial challenge for ceramic processing.

5. Conclusions

Sintered $YBa_2Cu_3O_{6+\delta}$ samples with different processing histories were prepared and their mechanical

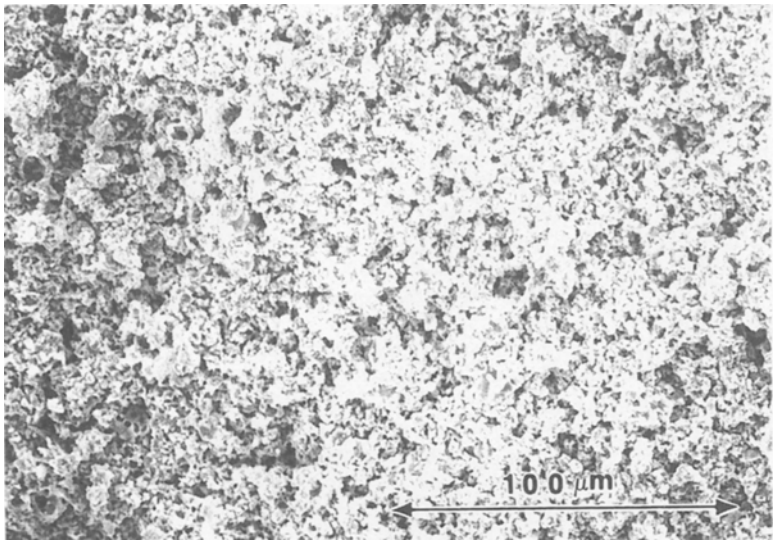

Figure 10 Scanning electron micrograph showing fracture surface of bar from set 53B (500 ×).

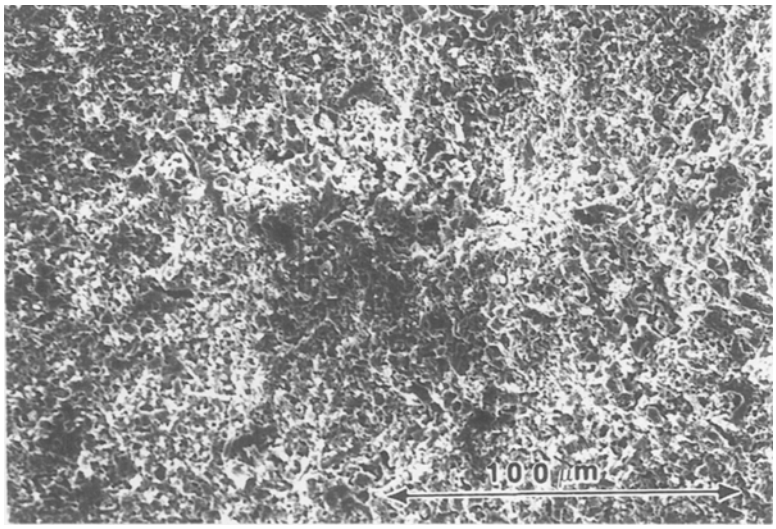

Figure 11 Scanning electron micrograph showing fracture surface of bar from set 54C (500 ×).

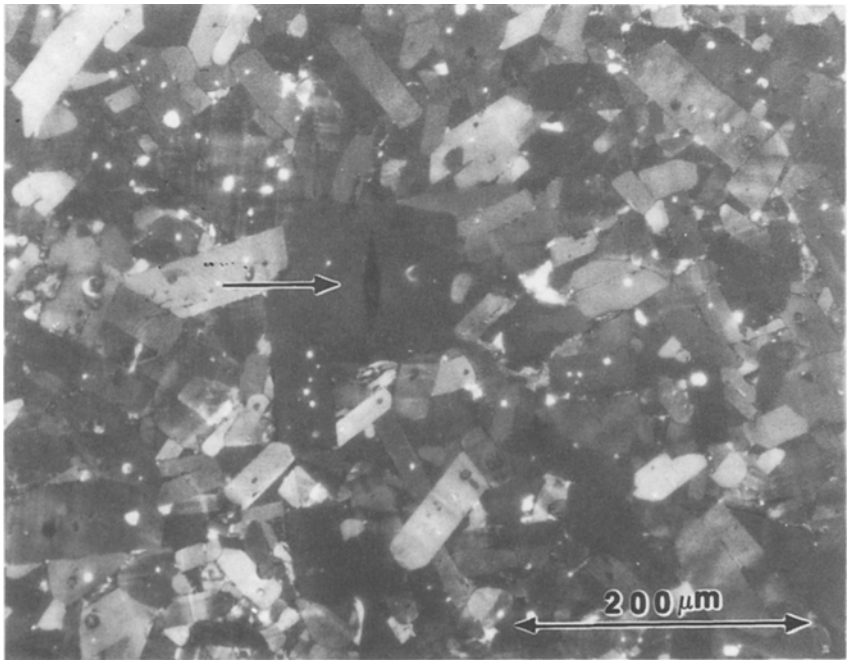

Figure 12 Optical micrograph of sample from set 35A(HT) showing microhardness indentation within a single $YBa_2Cu_3O_{6+\delta}$ grain (200 ×).

properties determined. The room-temperature flexural strength of $YBa_2Cu_3O_{6+\delta}$ ranged from 17.8 to 57.6 MPa for samples with densities ranging from 58 to 88% of theoretical density. The lowest-density samples showed the lowest strength. A set of samples with 76% density showed the greatest flexural strength, 57.6 MPa, possibly because of the presence of small amounts of additional phases, $BaCuO_2$ and Y_2BaCuO_5, which were identified in the samples. The flexural strength of $YBa_2Cu_3O_{6+\delta}$ at 77 K was 20% greater than the strength of similar samples measured at room temperature: 40.1 MPa compared with 33.8 MPa.

When samples of $YBa_2Cu_3O_{6+\delta}$ were exposed to air at 100% relative humidity at 38° C for 100 h, two layers of corrosion products formed: an outer, powdery layer of $BaCO_3$ and a near-surface layer containing CuO, $BaCO_3$ and Y_2BaCuO_5. The uncorroded core of the bars exhibited superconductivity and the same flexural strength as bars not exposed to moisture. This result suggests that despite the low density of the bars, corrosion is restricted to the surface and does not weaken the $YBa_2Cu_3O_{6+\delta}$ by penetrating the grain boundaries. Nevertheless, the extent of corrosion is such that some form of surface protection will be necessary for practical application of $YBa_2Cu_3O_{6+\delta}$.

The average microhardness of polycrystalline $YBa_2Cu_3O_{6+\delta}$, measured by the Knoop hardness method, ranged from 436 to 447 KHN. The average microhardness of large, individual grains of $YBa_2Cu_3O_{6+\delta}$ was 498 KHN.

Acknowledgements

The authors want to thank several colleagues in the General Motors Research Laboratories for their assistance throughout the course of this work: Jack Johnson for X-ray diffraction analysis, Noel Potter and Mike Balogh for chemical analysis, and Rick Waldo for microprobe analysis. The authors also acknowledge Jim Schroth and Alan Druschitz for helpful discussions and for reviewing this work. Alan Druschitz provided the silicon carbide test fixture upon which the flexural strength measurements were conducted.

References

1. A. P. MALOZEMOFF, W. J. GALLAGHER and R. E. SCHWALL, in "Chemistry of High-Temperature Superconductors", edited by D. L. Nelson, M. S. Whittingham and T. F. George (The American Chemical Society, Washington, DC, 1987) p. 280.
2. R. F. COOK, T. M. SHAW and P. R. DUNCOMBE, *Adv. Ceram. Mater.* **2** (1987) 606.
3. F. HELLMAN, E. M. GYORGY, D. W. JOHNSON, H. M. O'BRYAN and R. C. SHERWOOD, *J. Appl. Phys.* **63** (1988) 447.
4. "Flexural Strength of High Performance Ceramics at Ambient Temperature", MIL-STD-1942A (proposed). Director of the Army, Materials and Mechanics Research Centre, Attention AMXMR-SMS, Watertown MA, 02172-0001, November 1983.
5. A. F. MOHRNHEIM, in "Microhardness Testing, Interpretive Techniques for Microstructural Analysis" (Plenum, New York, 1977) p. 119.
6. W. B. KINGERY, H. K. BOWEN and D. UHLMANN, "Introduction to Ceramics", 2nd Ed (Wiley, New York, 1976) p. 791.
7. N. M. ALFORD, J. D. BIRCHALL, W. J. CLEGG, M. A. HARMER, K. KENDALL and D. H. JONES, *J. Mater. Sci.* **23** (1988) 761.
8. J. E. BLENDELL, C. K. CHIANG, D. C. CRANMER, S. W. FREIMAN, E. R. FULLER, E. DRESHER-KRASICKA, W. L. JOHNSON, H. M. LEDBETTER, L. H. BENNETT, L. J. SWARTZENDRUBER, R. B. MARINENKO, R. L. MYKLEBUST, D. S. BRIGHT and D. E. NEWBURY, in "Chemistry of High-Temperature Superconductors", edited by D. L. Nelson, M. S. Whittingham and T. F. George (American Chemical Society, Washington, DC, 1987) p. 240.
9. R. W. DAVIDGE, in "Mechanical Behaviour of Ceramics" (Cambridge University Press, Cambridge, 1979) p. 144.
10. N. D. PATEL, P. SARKAR, T. TROCZYNSKI, A. TAN and P. S. NICHOLSON, *Adv. Ceram. Mater.* **2** (1987) 617.
11. M. F. YAN, R. L. BARNS, H. M. O'BRYAN, P. K. GALLAGHER, R. C. SHERWOOD and S. JIN, *Appl. Phys. Lett.* **51** (1987) 532.
12. "Standard Methods for Determining the Average Grain Size", ASTM Standards, Designation E 112-85 (1985).
13. T. R. DINGER, T. K. WORTHINGTON, W. J. GALLAGHER and R. L. SANDSTROM, *Phys. Rev. Lett.* **58** (1987) 2687.
14. S. JIN, T. H. TIEFEL, R. C. SHERWOOD, R. B. van DOVER, M. E. DAVIS, G. W. KAMMLOTT and R. A. FASTNACHT, *Phys. Rev. B* **37** (1988) 7850.
15. D. DIMOS, P. CHAUDHARI, J. MANNHART and F. K. LeGOUES, *Phys. Rev. Lett.* **61** (1988) 219.
16. L. E. MURR, A. W. HARE and N. G. EROR, *Adv. Mater. Proc.* **132** (1987) 37.

Received 13 December 1988
and accepted 17 August 1989